

# A Framework for Characterising the Value of Information in Hidden Markov Models

Zijing Wang, *Student Member, IEEE*, Mihai-Alin Badiu, and Justin P. Coon, *Senior Member, IEEE*

**Abstract**—In this paper, a general framework is formalised to characterise the value of information (VoI) in hidden Markov models. Specifically, the VoI is defined as the mutual information between the current, unobserved status at the source and a sequence of observed measurements at the receiver, which can be interpreted as the reduction in the uncertainty of the current status given that we have noisy past observations of a hidden Markov process. We explore the VoI in the context of the noisy Ornstein-Uhlenbeck process and derive its closed-form expressions. Moreover, we study the effect of different sampling policies on VoI, deriving simplified expressions in different noise regimes and analysing the statistical properties of the VoI in the worst case. In simulations, the validity of theoretical results is verified, and the performance of VoI in the Markov and hidden Markov models is also analysed. Numerical results further illustrate that the proposed VoI framework can support the timely transmission in status update systems, and it can also capture the correlation property of the underlying random process and the noise in the transmission environment.

**Index Terms**—Value of information, age of information, hidden Markov models, Ornstein-Uhlenbeck process.

## I. INTRODUCTION

IN status update systems, sensor nodes are largely deployed to monitor different types of physical processes. They need to continuously sample data to get timely status updates about the targeted process, and the sampled data will be transmitted to the network to support real-time monitoring and control applications, such as environmental surveillance, smart transport, industrial control, e-health and so on. Stale data can be problematic. Therefore, the freshness of data plays an important role in such systems.

The age of information (AoI) has been introduced in [1], [2] as a new performance metric to characterise the data freshness from the receiver's perspective. It is defined as the time elapsed since the latest received status update was sampled. Specifically, the AoI at time  $t$  is given as

$$\Delta(t) = t - u(t), \quad (1)$$

where  $u(t)$  is the generation time of the latest sample received at the destination before time  $t$ . The AoI has received much attention due to its novelty of characterising the timeliness

This material is based upon work supported by, or in part by, the U. S. Army Research Laboratory and the U. S. Army Research Office under contract/grant number W911NF-19-1-0048. This work was also supported by EPSRC grant number EP/T02612X/1. The authors also gratefully acknowledge the support of the Clarendon Fund Scholarships at the University of Oxford. This paper was presented in part at the IEEE Global Communications Conference (GLOBECOM), Dec. 7-11, 2020.

The authors are with the Department of Engineering Science, University of Oxford, Oxford OX1 3PJ, U. K. (e-mail: {zijing.wang, mihai.badiu, and justin.coon}@eng.ox.ac.uk).

of information, and it has been widely studied as a concept, a metric, and a tool in a variety of communication systems [3], [4]. Many works focused on AoI and its variants in different queueing systems, studying statistical properties [1], [5], [6], and exploring the impact of queueing disciplines [7]–[9], transmission priority [10], packet deadlines [11], buffer sizes and packet replacement [12] on the performance of AoI. In addition to the fundamental-level research works, AoI-oriented scheduling and optimisation problems have also been extensively studied in the design of freshness-aware applications. Optimal link activation and sampling problems for AoI minimisation were investigated in single-hop [13] and multiple-hop networks [14]. AoI-based scheduling policies were proposed in [15], [16] to improve energy efficiency in energy harvesting networks. The joint optimisation of trajectory design and user scheduling problems were explored in unmanned aerial vehicle (UAV) networks [17], [18]. Furthermore, machine learning-based algorithms were applied to solve the above age-optimal problems more efficiently [19]–[21].

The age given in (1) increases linearly with time until a new status update is received which means that the concept of AoI is independent of the statistical variations inherent in the underlying source data. However, in some practical cases, old information with a large age may still have value while new information with a low age may have less value. For example, some information (e.g., the node mobility) update very frequently over time, thus even fresh samples may hold little valuable information; some other information (e.g., the temperature) update slowly, thus old samples may be sufficient enough to be used for further analysis. This means that the age of information cannot fully capture the performance degradation in information quality caused by the time lapse between status updates or the correlation property the underlying random process might exhibit. In this regard, it seems that AoI may not be a perfect metric. Therefore, more systematic approaches should be further investigated to quantify the information value.

A general way to measure the information value is to utilise the non-linear AoI functions [22]. The authors in [23] proposed the concept of the “age penalty”, which maps the AoI to a non-linear and non-decreasing penalty function to evaluate the level of “dissatisfaction” related to the outdated information. Closed-form expressions of non-linear age under different queueing models were derived in [24] for energy harvesting networks. The authors in [25] considered the auto-correlation of the random process and investigated exponential and logarithmic AoI penalty functions. Further-

more, information-theoretic AoI research has also been widely discussed to provide the theoretical interpretation of non-linear age functions. The mean square error (MSE) in remote estimation can remove the linearity and has been extensively utilised to measure the information value [26]–[31]. In [26], the authors defined a metric called the “effective age” which is increasing with the estimation error, and studied the optimal scheduling problem with the aim of minimising MSE for remote estimation of the Markov data source. The relationship between AoI and the estimation error was explored in the context of two Markov processes: Wiener process [27] and Ornstein-Uhlenbeck process [28]. In [29], the authors defined a context-aware metric called the “urgency of information” which can be used to describe both the non-linear performance degradation and the context dependence of the Markov status update system. The timely updating strategy for two correlated information sources was investigated in [30] to minimise the estimation error. Moreover, the conditional entropy was used in [32] to evaluate the staleness of data for estimation. In [33], the mutual information was utilised to characterise the timeliness of information, and the authors studied the optimal sampling policy for Markov models. Despite these contributions, hidden Markov models have not been explicitly treated in related works.

In practical applications, the noise, interference, errors or other features can lead to severe performance degradation. This means that the status updates generated at the source can be negatively affected, and may be hidden for observation when they are delivered to the receiver. However, existing works only treat Markov models in which variables are assumed to be directly visible at the destination node, and the timeliness of the system only relates to the most recent received status update.

Against this background, we are motivated to develop a general value of information (VoI) framework for hidden Markov models to characterise how valuable the status updates are at the receiver. In our previous work [34], we defined the basic notion of the information value and started to look at the Ornstein-Uhlenbeck (OU) process. In this paper, we extend the basic model and go into more depth with regard to different sampling policies. The contributions of this paper are given as follows:

- A VoI framework is formalised for hidden Markov models. The VoI is defined as the mutual information between the current status and a dynamic sequence of past observations, which gives the theoretical interpretation of the reduction in uncertainty in the current (unobserved) status of a hidden process given that we have noisy measurements.
- The VoI is explored in the context of one of the most important hidden Markov models: the noisy Ornstein-Uhlenbeck process, and its closed-form expressions are derived.
- The VoI with different sampling policies is investigated. For uniform sampling, simplified VoI expressions are derived in both large and small noise regimes. For random sampling, the simplified VoI expression is derived in the small noise regime, and the probability density and the

cumulative distribution of the worst-case VoI are analysed in a particular case: the M/M/1 queueing model.

- Numerical results are provided to verify the theoretical analysis. The effect of noise, number of observations, sampling rate and correlation on VoI and its statistical properties are discussed. The performance of VoI for Markov and hidden Markov models are also presented.

The remainder of this paper is organised as follows. The VoI formalism for hidden Markov models is given in Section II. The VoI for a specific hidden Markov model (the noisy OU process) is analysed in Section III. The VoI with uniform and random sampling policies are explored in Section IV and V, respectively. Numerical results and analysis are provided in Section VI. Conclusions are drawn in Section VII.

## II. VALUE OF INFORMATION FORMALISM

### A. Definition

We consider a status update system where the source node continuously monitors a random process and samples data to get timely status updates of the targeted process, and these time-stamped messages will be transmitted via the communication system to the destination node for further analysis. As the communication resources are limited, we assume that the transmission delay exists when the status updates are received by the destination.

We denote  $\{X_t\}$  as the random process under observation at the source node. Here, the time variable  $t$  can be either continuous or discrete. Denote  $(t_i, X_{t_i})$  as the message which is generated at arbitrary time  $t_i$ , and contains the corresponding value  $X_{t_i}$  of the underlying random process. The status update is received by the destination node at time  $t'_i$  with  $t'_i > t_i$ . The observations at the receiver are recorded in the observed random process  $\{Y_t\}$  where  $Y_{t'_i}$  is the observation corresponding to  $X_{t_i}$ . For the given time period  $(0, t)$ , denote  $n$  as the index of the most recent data received at time  $t'_n$  with  $t'_n < t \leq t'_{n+1}$ .

In this paper, we define the value of information as the mutual information between the current status of the underlying random process at the source and a dynamic sequence of past observations captured by the receiver. For the given time instants, the general definition of VoI is given as

$$v(t) = I(X_t; Y_{t'_n}, \dots, Y_{t'_{n-m+1}}), \quad t > t'_n, \quad (2)$$

which is conditioned on times  $\{t'_i\}$ . Here,  $n$  is the total number of recorded observations during the time period  $(0, t)$ . We look back in time and use a dynamic time window containing the most recent  $m$  of  $n$  samples ( $1 \leq m \leq n$ ) to measure the information value of the current status  $X_t$  of a hidden process.

### B. VoI for Hidden Markov Models

In the Markov model, the random process  $\{X_t\}$  is directly visible, and the observations are also Markovian, i.e.,  $Y_{t'_i} = X_{t_i}$ , for all  $1 \leq i \leq n$ . In this case, the VoI can be simplified to [33]

$$v(t) = I(X_t; X_{t_n}), \quad t > t'_n. \quad (3)$$

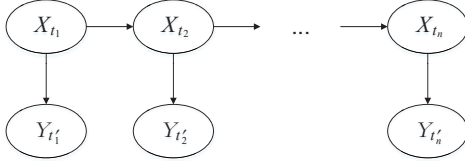


Fig. 1. Temporal evolution of hidden Markov models.

The VoI in the Markov model is independent of the length of time window  $m$  and only depends on the most recent single status update. For hidden Markov models (Fig. 1), the observations at the receiver may be different from the initial value, i.e.,  $Y_{t'_i} \neq X_{t_i}$ , but where

$$P[Y_{t'_i} \in A | X_{t_1}, \dots, X_{t_i}] = P[Y_{t'_i} \in A | X_{t_i}] \quad (4)$$

for all admissible  $A$ . Hence, the initial samples  $\{X_{t_i}\}$  are invisible at the receiver. In this case, we have

$$I(X_t; Y_{t'_n}, \dots, Y_{t'_{n-m+1}}) \geq I(X_t; Y_{t'_n}, \dots, Y_{t'_{n-m+2}}), \quad (5)$$

and

$$\begin{aligned} v(t) &= h(X_t) - h(X_t | Y_{t'_n}, \dots, Y_{t'_{n-m+1}}) \\ &\leq h(X_t) - h(X_t | Y_{t'_n}, \dots, Y_{t'_{n-m+1}}, X_{t_n}) \\ &= h(X_t) - h(X_t | X_{t_n}) \\ &= I(X_t; X_{t_n}) \end{aligned} \quad (6)$$

for  $2 \leq m \leq n$ . We find that the VoI increases with the length of the time window  $m$  and converges when more past observations are used. Moreover, the VoI in the Markov model can be regarded as the upper bound of the VoI in the hidden Markov model which illustrates that the lack of a direct route to observe  $\{X_t\}$  reduces the information value.

The difference between the VoI in the Markov model and its counterpart in the hidden Markov model can be expressed as

$$\begin{aligned} &I(X_t; X_{t_n}) - I(X_t; Y_{t'_n}, \dots, Y_{t'_{n-m+1}}) \\ &= h(X_t | Y_{t'_n}, \dots, Y_{t'_{n-m+1}}) - h(X_t | X_{t_n}) \\ &= h(X_t | Y_{t'_n}, \dots, Y_{t'_{n-m+1}}) - h(X_t | X_{t_n}, Y_{t'_n}, \dots, Y_{t'_{n-m+1}}) \\ &= I(X_t; X_{t_n} | Y_{t'_n}, \dots, Y_{t'_{n-m+1}}). \end{aligned} \quad (7)$$

This reduction can be interpreted as the ‘‘correction’’ which captures the VoI gap due to the indirect observation in the hidden Markov model. In other words, we can think the VoI for the hidden Markov model as the VoI for the Markov model minus the correction. The ‘‘correction’’ can be quantified by the mutual information between the current status  $X_t$  and the most recent (unobserved) status update  $X_{t_n}$  conditioned on the knowledge of a sequence of past observations  $\{Y_{t'_n}, \dots, Y_{t'_{n-m+1}}\}$ .

### III. VOI FOR A NOISY OU PROCESS

#### A. Noisy OU Process Model

In this section, we consider a particular case of a noisy Ornstein–Uhlenbeck process to show how the proposed VoI

framework can be applied in the hidden Markov model. The underlying OU process  $\{X_t\}$  satisfies the following stochastic differential equation (SDE)

$$dX_t = \kappa(\theta - X_t) dt + \sigma dW_t \quad (8)$$

where  $\{W_t\}$  is standard Brownian motion,  $\kappa$  is the rate of mean reversion,  $\theta$  is the long-term mean, and  $\sigma$  is the volatility of the random fluctuation. We assume that the initial value  $X_0$  is normally distributed with  $\mathcal{N}(\theta, \frac{\sigma^2}{2\kappa})$ . The OU process is a stationary Gauss–Markov process which can represent many practical applications. For example, it can be used to model the mobility of the node which is anchored to the point  $\theta$  but experiences positional disturbances.

For any  $t$ , the variable  $X_t$  is normally distributed with mean and variance:

$$E[X_t] = \theta, \quad \text{Var}[X_t] = \frac{\sigma^2}{2\kappa}. \quad (9)$$

$X_t$  conditioned on  $X_s$  is also Gaussian with mean and variance:

$$\begin{aligned} E[X_t | X_s] &= \theta + (X_s - \theta)e^{-\kappa(t-s)}, \\ \text{Var}[X_t | X_s] &= \frac{\sigma^2}{2\kappa} (1 - e^{-2\kappa(t-s)}). \end{aligned} \quad (10)$$

The covariance of two variables is given by

$$\text{Cov}[X_t, X_s] = \frac{\sigma^2}{2\kappa} e^{-\kappa|t-s|}. \quad (11)$$

We assume that the underlying OU process  $\{X_t\}$  is observed through an additive noise channel. Therefore, this noisy OU model constitutes a hidden Markov model with observations defined as

$$Y_{t'_i} = X_{t_i} + N_{t'_i}. \quad (12)$$

Here,  $\{N_t\}$  is a noise process which is anchored at time  $t'_i$  with the value  $N_{t'_i}$ . In practice, it can be used to represent the measurement or error that corrupts the status update  $X_{t_i}$ . We assume that  $\{N_{t'_i}\}$  are independent and identically distributed (i.i.d.) Gaussian variables with zero mean and constant variance  $\sigma_n^2$ . Let the  $m$ -dimensional vector  $\mathbf{X} = [X_{t_{n-m+1}}, \dots, X_{t_n}]^T$  denote the sequence of status updates sampled by the source node, and its covariance matrix is given by

$$\begin{aligned} \Sigma_{\mathbf{X}} &= \\ &\left[ \begin{array}{ccc} \text{Cov}[X_{t_{n-m+1}}, X_{t_{n-m+1}}] & \cdots & \text{Cov}[X_{t_{n-m+1}}, X_{t_n}] \\ \vdots & \ddots & \vdots \\ \text{Cov}[X_{t_{n-m+1}}, X_{t_n}] & \cdots & \text{Cov}[X_{t_n}, X_{t_n}] \end{array} \right]. \end{aligned} \quad (13)$$

Let vector  $\mathbf{Y} = [Y_{t'_{n-m+1}}, \dots, Y_{t'_n}]^T$  denote the corresponding set of observations recorded at the receiver. Similarly, the associated noise samples are captured in vector  $\mathbf{N} = [N_{t'_{n-m+1}}, \dots, N_{t'_n}]^T$  with the covariance matrix

$$\Sigma_{\mathbf{N}} = \sigma_n^2 \mathbf{I}, \quad (14)$$

where  $\mathbf{I}$  is the identity matrix. Therefore, the observations of the noisy OU process can be collectively represented by

$$\mathbf{Y} = \mathbf{X} + \mathbf{N}. \quad (15)$$

### B. VoI for the Noisy OU Process

Based on the model given before, we can state the following main result of this section.

**Proposition 1.** *Let the  $m$ -dimensional matrix  $\mathbf{A} = \sigma_n^2 \Sigma_{\mathbf{X}}^{-1} + \mathbf{I}$ , and denote  $\mathbf{A}_{ij}$  as the  $(m-1) \times (m-1)$  matrix constructed by removing the  $i$ th row and the  $j$ th column of the matrix  $\mathbf{A}$ . The VoI for the noisy OU process defined above can be written as*

$$v(t) = \frac{1}{2} \log \left( \frac{1}{1 - e^{-2\kappa(t-t_n)}} \right) - \frac{1}{2} \log \left( 1 + \frac{1}{(e^{2\kappa(t-t_n)} - 1)} \frac{\det(\mathbf{A}_{mm})}{\gamma \det(\mathbf{A})} \right). \quad (16)$$

Here,  $\gamma$  is denoted as the ratio of the variance of the OU process and the variance of the noise, i.e.,

$$\gamma = \frac{\text{Var}[X_{t_i}]}{\text{Var}[N_{t'_i}]} = \frac{\sigma^2}{2\kappa\sigma_n^2}. \quad (17)$$

*Proof:* See appendix A.  $\blacksquare$

It is easy to show that the first logarithmic term in (16) represents the VoI for the Markov OU model  $X_t$ . The remainder quantifies a ‘‘correction’’ to the VoI of the hidden process that arises due to the indirect observation of the process through the noisy channel, and it evaluates the result of (7) in the example of the OU model. Note that both  $\mathbf{A}$  and  $\mathbf{A}_{mm}$  are positive semi-definite, thus the second logarithmic term in (16) is non-negative. The parameter  $\gamma$  gives a comparison between the randomness in the underlying OU process and the noise process in the communication channel, and it can be compared to the concept of the signal-to-noise ratio (SNR) in communication systems.

### C. Results for a Single Observation

The result given in Proposition 1 is general. In this subsection, we consider a special case ( $m = 1$ ) which gives the information about how much value the most recently received observation contains about the current status of a random process. In this case, the VoI can be calculated by replacing the  $m$ -dimensional vector  $\mathbf{Y}$  with the single variable  $Y_{t'_n}$  in (2), which leads to the following corollary.

**Corollary 1.** *The VoI for the noisy OU process with a single observation is given by*

$$v(t) = -\frac{1}{2} \log \left( 1 - \frac{\gamma}{1 + \gamma} e^{-2\kappa(t-t_n)} \right). \quad (18)$$

*Proof:* This result follows directly from Proposition 1 where  $\det(\mathbf{A}_{mm}) := 1$ .  $\blacksquare$

This corollary shows that for fixed  $t_n$ , as time  $t$  increases, the VoI will decrease and the newly received update can cause a corresponding reset of  $v(t)$ . This is somewhat similar to the concept of AoI, which is equal to  $t'_n - t_n$  at the moment the  $n$ th update arrives and then increases with unit slope until the next update comes. However, the VoI will decrease like  $O(e^{-2\kappa t})$  until a new status update is received. The parameter  $\kappa$  can be used to represent how correlated the updates are. Therefore, compared with AoI, the proposed VoI framework

not only reflects the time evolution of a random process, but also captures the correlation property of the underlying data source and the noise in the transmission channel.

### IV. NOISY OU MODEL WITH UNIFORM SAMPLING

Corollary 1 looks at the special case when the length of the time window  $m = 1$  to illustrate the VoI concept clearly. When  $m > 1$ , the covariance matrix  $\Sigma_{\mathbf{X}}$  given in Proposition 1 is closely related to the sampling interval of the status updates. To explore this result further, we will study how the sampling policy affects the VoI. We first consider the case when the sampling intervals are uniform in this section.

We assume that status updates of the OU process under observation are generated at regular times  $t_i = i\Delta t$ , where the constant  $\Delta t$  ( $\Delta t > 0$ ) denotes the fixed sampling interval. For the OU process with uniform sampling, the  $m$  samples in  $\mathbf{X}$  form a first-order autoregressive AR(1) process. Let  $\rho = e^{-\kappa\Delta t}$ . The inverse covariance matrix of  $\mathbf{X}$  is a tridiagonal matrix which is written as [35]

$$\Sigma_{\mathbf{X}}^{-1} = \frac{2\kappa}{\sigma^2(1 - \rho^2)} \begin{bmatrix} 1 & -\rho & & & \\ -\rho & 1 + \rho^2 & -\rho & & \\ & -\rho & \ddots & \ddots & \\ & & \ddots & 1 + \rho^2 & -\rho \\ & & & -\rho & 1 \end{bmatrix}. \quad (19)$$

Then the matrix  $\mathbf{A}$  in Proposition 1 is given by

$$\mathbf{A} = \sigma_n^2 \Sigma_{\mathbf{X}}^{-1} + \mathbf{I} = \begin{bmatrix} a & b & & & \\ b & c & b & & \\ & b & \ddots & \ddots & \\ & & \ddots & c & b \\ & & & b & a \end{bmatrix}, \quad (20)$$

where

$$a = \frac{1}{\gamma(1 - \rho^2)} + 1, \quad b = \frac{-\rho}{\gamma(1 - \rho^2)}, \quad c = \frac{1 + \rho^2}{\gamma(1 - \rho^2)} + 1. \quad (21)$$

It is clear to see that the matrix  $\mathbf{A}$  is also tridiagonal, so its determinant can be calculated by cofactor expansion and be expressed by a recurrence relation [36]. Therefore, in this case, we have

$$\det(\mathbf{A}) = \frac{(-1)^m b^{m-1}}{\sqrt{c^2 - 4b^2}} \left( a^2(\lambda_1^{m-1} - \lambda_2^{m-1}) + 2ab(\lambda_1^{m-2} - \lambda_2^{m-2}) + b^2(\lambda_1^{m-3} - \lambda_2^{m-3}) \right) \quad (22)$$

$$\det(\mathbf{A}_{mm}) = \frac{(-1)^{m-1} b^{m-2}}{\sqrt{c^2 - 4b^2}} \left( ac(\lambda_1^{m-2} - \lambda_2^{m-2}) + (ab + bc)(\lambda_1^{m-3} - \lambda_2^{m-3}) + b^2(\lambda_1^{m-4} - \lambda_2^{m-4}) \right) \quad (23)$$

where

$$\lambda_1 = \frac{-c + \sqrt{c^2 - 4b^2}}{2b}, \quad \lambda_2 = \frac{-c - \sqrt{c^2 - 4b^2}}{2b}. \quad (24)$$

*Proof:* See appendix B.  $\blacksquare$

$$\frac{\det(\mathbf{A}_{mm})}{\gamma \det(\mathbf{A})} = \frac{1 - \rho^2}{\rho} \cdot \frac{ac(\lambda_1^{m-2} - \lambda_2^{m-2}) + (ab + bc)(\lambda_1^{m-3} - \lambda_2^{m-3}) + b^2(\lambda_1^{m-4} - \lambda_2^{m-4})}{a^2(\lambda_1^{m-1} - \lambda_2^{m-1}) + 2ab(\lambda_1^{m-2} - \lambda_2^{m-2}) + b^2(\lambda_1^{m-3} - \lambda_2^{m-3})} \quad (25)$$

Thus, we have derived the closed-form expression of the determinant ratio in (25), which can help further explore how the VoI relates to the sampling interval  $\Delta t$ , correlation parameter  $\kappa$  and channel condition parameter  $\sigma_n^2$ .

### A. High SNR Regime

The parameter  $\gamma$  given in (17) can largely affect the VoI in the hidden Markov model. If  $\gamma$  is large, the underlying latent process is dominant; otherwise, the noise process is dominant. Therefore, it is interesting to explore the VoI with different levels of noise. In this subsection, we consider the high SNR regime in which the small variance of noise leads to large  $\gamma$ , i.e.,  $\frac{1}{\gamma} \rightarrow 0$ . In this case, we can state the following result.

**Corollary 2.** *For the noisy OU process with uniform sampling, the VoI in the high SNR regime can be given as*

$$v(t) = \frac{1}{2} \log \left( \frac{1}{1 - e^{-2\kappa(t-t_n)}} \right) - \frac{1}{2} \log \left[ 1 + \frac{1}{e^{2\kappa(t-t_n)} - 1} \left( \frac{1}{\gamma} - \frac{1}{(1 - \rho^2)\gamma^2} \right) \right] + O\left(\frac{1}{\gamma^3}\right). \quad (26)$$

*Proof:* We substitute (21) and (24) into (25), and expand this expression at the point  $\frac{1}{\gamma} = 0$ . Hence, the series expansion of (25) in the high SNR regime can be given as

$$\frac{\det(\mathbf{A}_{mm})}{\gamma \det(\mathbf{A})} = \frac{1}{\gamma} - \frac{1}{(1 - \rho^2)\gamma^2} + O\left(\frac{1}{\gamma^3}\right). \quad (27)$$

In this case, the VoI ‘‘correction’’ can be written as

$$\begin{aligned} & \frac{1}{2} \log \left( 1 + \frac{1}{(e^{2\kappa(t-t_n)} - 1)} \frac{\det(\mathbf{A}_{mm})}{\gamma \det(\mathbf{A})} \right) \\ &= \frac{1}{2} \log \left[ 1 + \frac{1}{e^{2\kappa(t-t_n)} - 1} \left( \frac{1}{\gamma} - \frac{1}{(1 - \rho^2)\gamma^2} + O\left(\frac{1}{\gamma^3}\right) \right) \right] \\ &= \frac{1}{2} \log \left[ 1 + \frac{1}{e^{2\kappa(t-t_n)} - 1} \left( \frac{1}{\gamma} - \frac{1}{(1 - \rho^2)\gamma^2} \right) \right] \\ & \quad + \frac{1}{2} \log \left[ 1 + \frac{O\left(\frac{1}{\gamma^3}\right)}{1 + \frac{1}{e^{2\kappa(t-t_n)} - 1} \left( \frac{1}{\gamma} - \frac{1}{(1 - \rho^2)\gamma^2} \right)} \right] \\ &= \frac{1}{2} \log \left[ 1 + \frac{1}{e^{2\kappa(t-t_n)} - 1} \left( \frac{1}{\gamma} - \frac{1}{(1 - \rho^2)\gamma^2} \right) \right] + O\left(\frac{1}{\gamma^3}\right). \end{aligned} \quad (28)$$

Therefore, the result of this corollary is obtained directly by substituting (28) into (16). ■

Similar to Proposition 1, the first logarithmic term in Corollary 2 represents the VoI for the non-noisy Markov OU process  $\{X_t\}$ , and the remainder quantifies the ‘‘correction’’ which can be presented as the scale of  $\frac{1}{\gamma}$ . We find that the expression of  $v(t)$  does not depend on  $m$  (the number of samples are used). This is because when  $\gamma$  is large, the Markov OU randomness is dominant, and the noisy channel is not expected to play a vital role in the calculation of VoI. Therefore, the VoI in the high

SNR regime approaches its Markov counterpart which is not related to  $m$ . Furthermore, if the VoI given in (26) is truncated to the second-order term  $\frac{1}{\gamma^2}$ , the approximated VoI will first decrease and then increase with  $\frac{1}{\gamma}$ . The turning point is at  $\frac{1}{\gamma} = \frac{1 - \rho^2}{2}$ . Therefore, the valid region of the approximated VoI is

$$\gamma \geq \frac{2}{1 - \rho^2}. \quad (29)$$

### B. Low SNR Regime

The VoI in the low SNR regime (i.e.,  $\gamma \rightarrow 0$ ) can be obtained similarly. We have the following result of this subsection.

**Corollary 3.** *For the noisy OU process with uniform sampling, the VoI in the low SNR regime can be given as*

$$\begin{aligned} v(t) = & -\frac{1}{2} \log \left[ 1 - \frac{e^{-2\kappa(t-t_n)}(1 - \rho^{2m})}{1 - \rho^2} \gamma + e^{-2\kappa(t-t_n)} \right. \\ & \times \left. \left( \frac{(1 - \rho^{2m})(1 + \rho^2)}{(1 - \rho^2)^2} - \frac{2m\rho^{2m}}{1 - \rho^2} \right) \gamma^2 \right] + O(\gamma^3). \end{aligned} \quad (30)$$

*Proof:* The series expansion of (25) at the point  $\gamma = 0$  can be written as

$$\begin{aligned} \frac{\det(\mathbf{A}_{mm})}{\gamma \det(\mathbf{A})} = & 1 - \frac{1 - \rho^{2m}}{1 - \rho^2} \gamma \\ & + \left( \frac{(1 - \rho^{2m})(1 + \rho^2)}{(1 - \rho^2)^2} - \frac{2m\rho^{2m}}{1 - \rho^2} \right) \gamma^2 + O(\gamma^3). \end{aligned} \quad (31)$$

Similar to the proof given in Corollary 2, the result of this corollary given in (30) is obtained by substituting (31) into (16). ■

The VoI in the low SNR regime is presented as the scale of  $\gamma$ . Compared with the high SNR regime, the randomness of the noise dominates in the low SNR regime, thus the VoI relates to the length of the time window  $m$ . As  $0 < \rho < 1$ , the result in this corollary further shows that the VoI increases with  $m$  and converges when  $m$  grows large. Moreover, if we omit the term  $O(\gamma^3)$  in (30), the valid region of the approximated VoI in the low SNR regime can be given by

$$\gamma \leq \frac{(1 - \rho^2)(1 - \rho^{2m})}{2(1 - \rho^{2m})(1 + \rho^2) - 4m\rho^2(1 - \rho^2)}. \quad (32)$$

## V. NOISY OU MODEL WITH RANDOM SAMPLING

In some cases, the status update may not be generated with uniform time intervals. In such applications, it may still be of interest to have a clear representation of VoI with irregular sampling intervals. In this section, we consider a more general case for the VoI in the noisy OU process with a random sampling policy.

We assume that status updates are generated as a rate  $\lambda$  Poisson process and let the i.i.d. exponential random variables

$$T_i = t_{n-m+i} - t_{n-m+i-1}, \quad 2 \leq i \leq m \quad (33)$$

be the sampling interval of two packets. In this case, the covariance matrix of  $\mathbf{X}$  can be written as

$$\Sigma_{\mathbf{X}} = \frac{\sigma^2}{2\kappa} \begin{bmatrix} 1 & e^{-\kappa T_2} & \cdots & e^{-\kappa \sum_{i=2}^m T_i} \\ e^{-\kappa T_2} & 1 & \cdots & e^{-\kappa \sum_{i=3}^m T_i} \\ \vdots & \vdots & \ddots & \vdots \\ e^{-\kappa \sum_{i=2}^m T_i} & e^{-\kappa \sum_{i=3}^m T_i} & \cdots & 1 \end{bmatrix}. \quad (34)$$

For simplicity, let the random variable

$$R_i = \frac{1}{1 - e^{-2\kappa T_i}}, \quad 2 \leq i \leq m. \quad (35)$$

The inverse of the covariance matrix of  $\mathbf{X}$  is tridiagonal which can be written as [35], [37]

$$\Sigma_{\mathbf{X}}^{-1} = \frac{2\kappa}{\sigma^2} \begin{bmatrix} a_1 & b_1 & & & \\ b_1 & a_2 & b_2 & & \\ & b_2 & \ddots & \ddots & \\ & \ddots & a_{m-1} & b_{m-1} & \\ & & b_{m-1} & a_m & \end{bmatrix}, \quad (36)$$

where

$$a_i = \begin{cases} R_2 & i = 1 \\ R_m & i = m \\ R_i + R_{i+1} - 1 & \text{others} \end{cases} \quad (37)$$

and

$$b_i = -\sqrt{R_{i+1}(R_{i+1} - 1)}, \quad 1 \leq i \leq m-1. \quad (38)$$

Then, the matrix  $\mathbf{A}$  in Proposition 1 can be written as

$$\mathbf{A} = \sigma_n^2 \Sigma_{\mathbf{X}}^{-1} + \mathbf{I} = \begin{bmatrix} \frac{1}{\gamma} a_1 + 1 & \frac{1}{\gamma} b_1 & & & \\ \frac{1}{\gamma} b_1 & \frac{1}{\gamma} a_2 + 1 & \frac{1}{\gamma} b_2 & & \\ & \frac{1}{\gamma} b_2 & \ddots & \ddots & \\ & \ddots & \frac{1}{\gamma} a_{m-1} + 1 & \frac{1}{\gamma} b_{m-1} & \\ & & \frac{1}{\gamma} b_{m-1} & \frac{1}{\gamma} a_m + 1 & \end{bmatrix}. \quad (39)$$

#### A. VoI in the High SNR Regime

Similar to our analysis in Sec. IV, we consider the high SNR regime (i.e.,  $\frac{1}{\gamma} \rightarrow 0$ ) to simplify the expression of the VoI with random sampling.

**Lemma 1.** *Let  $f_i$  denote the determinant of the  $i$ -dimensional matrix constructed from the first  $i$  columns and rows of matrix  $\mathbf{A}$ , i.e.,  $f_{m-1} = \det(\mathbf{A}_{mm})$  and  $f_m = \det(\mathbf{A})$ . In the high SNR regime,  $f_k$  can be calculated as*

$$f_k = 1 + \sum_{i=1}^k a_i \frac{1}{\gamma} + \left( \sum_{1 \leq i < j \leq k} a_i a_j - \sum_{i=1}^{k-1} b_i^2 \right) \frac{1}{\gamma^2} + O\left(\frac{1}{\gamma^3}\right) \quad (40)$$

for  $1 < k \leq m$ .  $\blacksquare$

*Proof:* See appendix C.

Then, we have the following corollary.

**Corollary 4.** *For the noisy OU process with random sampling, the VoI in the high SNR regime can be written as*

$$v(t) = \frac{1}{2} \log \left( \frac{1}{1 - e^{-2\kappa(t-t_n)}} \right) - \frac{1}{2} \log \left[ 1 + \frac{1}{e^{2\kappa(t-t_n)} - 1} \right. \\ \left. \times \left( \frac{1}{\gamma} - \frac{1}{1 - e^{-2\kappa(t_n-t_{n-1})}} \frac{1}{\gamma^2} \right) \right] + O\left(\frac{1}{\gamma^3}\right). \quad (41)$$

*Proof:* For simplicity, we temporarily denote the coefficient of the second-order term  $\frac{1}{\gamma^2}$  in (40) as  $c_k$ , i.e.,

$$c_k = \sum_{1 \leq i < j \leq k} a_i a_j - \sum_{i=1}^{k-1} b_i^2. \quad (42)$$

Based on Lemma 1, we have

$$\frac{\det(\mathbf{A}_{mm})}{\gamma \det(\mathbf{A})} = \frac{1}{\gamma} \cdot \frac{1 + \sum_{i=1}^{m-1} a_i \frac{1}{\gamma} + c_{m-1} \frac{1}{\gamma^2} + O\left(\frac{1}{\gamma^3}\right)}{1 + \sum_{i=1}^m a_i \frac{1}{\gamma} + c_m \frac{1}{\gamma^2} + O\left(\frac{1}{\gamma^3}\right)} \\ = \frac{1}{\gamma} - a_m \frac{1}{\gamma^2} + (b_{m-1}^2 - a_m^2) \frac{1}{\gamma^3} + O\left(\frac{1}{\gamma^4}\right) \\ = \frac{1}{\gamma} - R_m \frac{1}{\gamma^2} - R_m \frac{1}{\gamma^3} + O\left(\frac{1}{\gamma^4}\right) \\ = \frac{1}{\gamma} - \frac{1}{1 - e^{-2\kappa(t_n-t_{n-1})}} \frac{1}{\gamma^2} + O\left(\frac{1}{\gamma^3}\right). \quad (43)$$

Similar to the proof given in Corollary 2, the result of this corollary given in (41) is obtained by substituting (43) into (16).  $\blacksquare$

In the high SNR regime, the VoI with random sampling shows the similar behaviours as its counterpart with uniform sampling in Corollary 2. The expression of  $v(t)$  does not depend on the number of samples used due to the dominant Markov OU randomness. For random sampling, the ‘‘correction’’ term is also presented as the scale of  $\frac{1}{\gamma}$  and it relates to the time difference  $t_n - t_{n-1}$  which is a random variable. Furthermore, if the VoI given in (41) is truncated to the second-order term  $\frac{1}{\gamma^2}$ , the approximated VoI in Corollary 4 is valid when

$$\gamma \geq \frac{2}{1 - e^{-2\kappa(t_n-t_{n-1})}}. \quad (44)$$

#### B. An Application of VoI in the M/M/1 System

In this subsection, we consider the case of a first-come-first-serve (FCFS) M/M/1 queueing system to explore the statistical property of the VoI, which provides the potential applicability of the proposed framework.

We assume that status updates are sampled as a rate  $\lambda$  Poisson process and the service rate is  $\mu$ . Let the random variables

$$T_i = t_i - t_{i-1}, \quad n - m + 2 \leq i \leq n \quad (45)$$

be the sampling interval of two packets, which are i.i.d. exponential random variables with mean  $\frac{1}{\lambda}$  and variance  $\frac{1}{\lambda^2}$ .

Let the random variables  $\{W_i\}$  ( $n-m+1 \leq i \leq n$ ) be the service time which are i.i.d. exponential random variables with mean  $\frac{1}{\mu}$  and variance  $\frac{1}{\mu^2}$ . Let the random variable

$$S_i = t'_i - t_i, \quad n-m+1 \leq i \leq n \quad (46)$$

be the system time of the  $i$ th status update. When the system reaches steady state, the system times are also i.i.d. exponential random variables with the mean  $1/(\mu - \lambda)$  [1], [38].

We consider the case when  $m = 1$  and the VoI expression is given in Corollary 1. We observe that the VoI immediately reaches the local minimum before a new update is received by the destination. Given that  $n$  samples are observed, the worst-case VoI can be obtained when  $t = t'_{n+1}$  and it is believed to be of interest in applications with a threshold restriction on the information value. When the time instants are random, the VoI in the worst case can also be regarded as a random variable. Based on (18), the worst VoI with  $n$  status updates is given as

$$\begin{aligned} V_n &= -\frac{1}{2} \log \left( 1 - \frac{\gamma}{1+\gamma} e^{-2\kappa(t'_{n+1} - t_n)} \right) \\ &= -\frac{1}{2} \log \left( 1 - \frac{\gamma}{1+\gamma} e^{-2\kappa((t'_{n+1} - t_{n+1}) + (t_{n+1} - t_n))} \right) \\ &= -\frac{1}{2} \log \left( 1 - \frac{\gamma}{1+\gamma} e^{-2\kappa(S_{n+1} + T_{n+1})} \right). \end{aligned} \quad (47)$$

The system time  $S_{n+1}$  and the sampling interval  $T_{n+1}$  are the main factors affecting the distribution of VoI. The joint probability density function (PDF) of  $S_{n+1}$  and  $T_{n+1}$  is given by

$$f_{T,S}(t, s) = \lambda \mu e^{-\lambda t - \mu s} - \mu^2 e^{-\mu(t+s)} + \mu(\mu - \lambda) e^{-\mu t - (\mu - \lambda)s}. \quad (48)$$

*Proof:* See appendix D.  $\blacksquare$

Let the variable  $Z_{n+1} = S_{n+1} + T_{n+1}$  and its PDF is given by

$$f_Z(z) = \int_0^z f_{T,S}(z-s, s) ds = \mu \left[ \frac{\lambda}{\mu - \lambda} e^{-\lambda z} - \left( \frac{\lambda}{\mu - \lambda} + \mu z + \frac{\mu - \lambda}{\lambda} \right) e^{-\mu z} + \frac{\mu - \lambda}{\lambda} e^{-(\mu - \lambda)z} \right]. \quad (49)$$

Let the monotonic function

$$g(z) = -\frac{1}{2} \log \left( 1 - \frac{\gamma}{1+\gamma} e^{-2\kappa z} \right). \quad (50)$$

Then, the PDF of  $V_n$  can be calculated as

$$f_V(v) = f_Z(g^{-1}(v)) \left| \frac{d}{dv} (g^{-1}(v)) \right|. \quad (51)$$

Here, the  $g^{-1}$  denotes the inverse function, and we have

$$g^{-1}(v) = -\frac{1}{2\kappa} \log \left( \frac{(1+\gamma)(1-e^{-2v})}{\gamma} \right), \quad (52)$$

$$\frac{d}{dv} (g^{-1}(v)) = -\frac{e^{-2v}}{\kappa(1-e^{-2v})}. \quad (53)$$

Then, we can state the following results.

**Proposition 2.** In the FCFS M/M/1 queueing system, the probability density function of the worst-case VoI is given by

$$f_V(v) = \frac{\mu e^{-2v}}{\kappa(1-e^{-2v})} \left[ \frac{\lambda}{\mu - \lambda} (r(v))^{\frac{\lambda}{2\kappa}} - \left( \frac{\lambda}{\mu - \lambda} + \frac{\mu - \lambda}{2\kappa} \log(r(v)) \right) (r(v))^{\frac{\mu}{2\kappa}} + \frac{\mu - \lambda}{\lambda} (r(v))^{\frac{\mu - \lambda}{2\kappa}} \right]. \quad (54)$$

Here,  $r(v)$  is denoted as

$$r(v) = \frac{(1+\gamma)(1-e^{-2v})}{\gamma}. \quad (55)$$

*Proof:* This result is obtained directly by substituting (49), (52) and (53) into (51).  $\blacksquare$

**Proposition 3.** In the FCFS M/M/1 queueing system, the cumulative distribution function of the worst-case VoI is given by

$$\begin{aligned} F_V(v) &= P(V \leq v) = \frac{(\mu - \lambda)}{\mu} e^{-\frac{v\lambda}{\kappa}} (r(v))^{\frac{\lambda}{2\kappa}(1+\frac{2v}{\log(r(v))})} \\ &\quad + \frac{\lambda}{\mu} e^{-\frac{v(\mu-\lambda)}{\kappa}} (r(v))^{\frac{\mu-\lambda}{2\kappa}(1+\frac{2v}{\log(r(v))})} \\ &+ \left( 1 - \frac{\mu^2}{\lambda(\mu - \lambda)} + \frac{\mu}{2\kappa} \log(r(v)) \right) e^{-\frac{v\mu}{\kappa}} (r(v))^{\frac{\mu}{2\kappa}(1+\frac{2v}{\log(r(v))})}. \end{aligned} \quad (56)$$

*Proof:* The cumulative distribution function (CDF) is obtained directly by

$$F_V(v) = \int_0^v f_V(x) dx. \quad (57)$$

In practice, this distribution function can be interpreted as the “VoI outage”, i.e., the probability that the VoI right before a new sample arrives is below a threshold  $v$ , which can play a vital role in the system design.

## VI. NUMERICAL RESULTS

In this section, numerical results are provided through Monte Carlo simulations. Results show the VoI performance in the Markov and hidden Markov models, verify the validity of the simplified VoI in the high and low SNR regimes and illustrate the effect of time window’s length, sampling rate, correlation and noise on the VoI. In the simulation, the long-term mean parameter  $\sigma$  of the OU model is set as 1. We consider the FCFS transmission and the service time of each status update is generated randomly by a rate  $\mu = 1$  exponential distribution.

Fig. 2 shows the VoI in the Markov and hidden Markov OU models for different length of time window  $m$ . In the noisy OU process, all the received observations are used for the result labelled “ $m = n$ ”; only the most recent received single observation is used for the result labelled “ $m = 1$ ”. This figure verifies the results given in Proposition 1 and Corollary 1. The VoI decreases with time until a new update is transmitted which shows the similar behaviour to the traditional AoI evolution. The black curve represents the VoI in the underlying

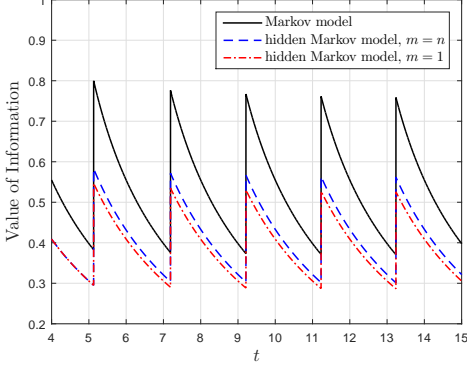


Fig. 2. Time evolution of VoI in Markov OU process and the noisy OU process; correlation parameter  $\kappa = 0.1$ , noise parameter  $\sigma_n^2 = 1$  and sampling interval  $\Delta t = 2$ .

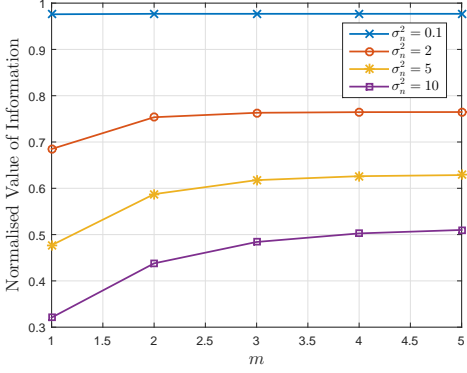


Fig. 3. VoI in the noisy OU process versus the length of the time window  $m$  for  $\sigma_n^2 \in \{0.1, 2, 5, 10\}$  at  $t = 100$ ; correlation parameter  $\kappa = 0.05$  and sampling interval  $\Delta t = 2$ .

Markov OU model which is the first term in Proposition 1. The gap between the result in the Markov model and its counterpart in the hidden Markov model is the second term in Proposition 1 which represents the ‘‘VoI correction’’ due to the indirect observation. Furthermore, the gap between two curves in the hidden Markov model increases with time. This means that the length of the time window can affect the VoI in the hidden Markov model. However, the VoI in the Markov model does not depend on  $m$ .

Fig. 3 further shows how the VoI varies with the length of the time window  $m$  for different values of  $\sigma_n^2$ . The horizontal axis represents the number of observations we used to predict the value of the current status of the random process. The vertical axis is the normalised VoI which represents the ratio of  $v(t)$  to  $v_{OU}(t)$ , where  $v_{OU}(t)$  is the VoI in the underlying Markov OU process. This result shows that the VoI in the noisy OU process increases with the length of the time window, and converges as more past observations are used. This can be explained as more past observations can give more information about the current status of the latent random process. Moreover, the normalised VoI is approaching 1 for small  $\sigma_n^2$  which means that the VoI in the Markov model can be regarded as the upper bound of its counterpart in the hidden

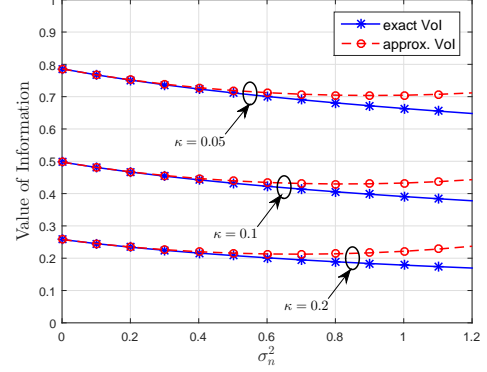


Fig. 4. High SNR regime: Comparison of the exact VoI and the approximated VoI with uniform sampling for  $\kappa \in \{0.05, 0.1, 0.2\}$  at  $t = 100$ ; sampling interval  $\Delta t = 2$  and the length of time window  $m = 5$ .

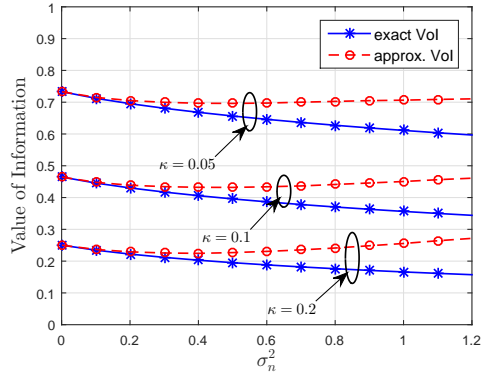


Fig. 5. High SNR regime: Comparison of the exact VoI and the approximated VoI with random sampling for  $\kappa \in \{0.05, 0.1, 0.2\}$  at  $t = 100$ ; sampling rate  $\lambda = 0.5$  and the length of time window  $m = 5$ .

Markov model (6).

Fig. 4, 5 and 6 show the numerical validation of the exact general VoI given in Proposition 1 and the approximated VoI with different sampling policies in different SNR regimes which are discussed in Corollaries 2, 3 and 4. Fig. 4 and 5 consider the high SNR regime with uniform and random sampling policies, respectively. We compare the exact VoI given in (16) with the approximated VoI in the high SNR regime given in (26) and (41), respectively. It is not surprising that the exact VoI decreases as  $\sigma_n^2$  increases. As the approximated VoI is truncated to the second-order term of  $\frac{1}{\gamma}$ , the VoI first decreases and starts to increase when it reaches the invalid region as  $\sigma_n^2$  increases. The turning points are  $\sigma_n^2 \in \{0.9, 0.8, 0.7\}$  in Fig. 4 and  $\{0.5, 0.4, 0.3\}$  in Fig. 5, verifying the results given in (29) and (44). As expected, the approximated VoI is very close to the actual VoI when  $\sigma_n^2$  and  $\kappa$  are small, while the gap increases when the system experiences larger noise. Fig. 6 considers the low SNR regime, and compares the exact VoI with the approximated VoI given in (30). Compared to the high SNR regime, we observe the opposite behaviour, i.e., the approximated VoI is approaching the exact VoI when  $\sigma_n^2$  and  $\kappa$  are large. Therefore, these simulation results verify the analysis in Corollaries 2, 3 and 4.

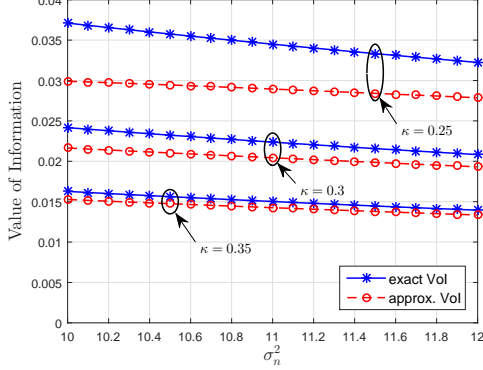


Fig. 6. Low SNR regime: Comparison of the exact VoI and the approximated VoI with uniform sampling for  $\kappa \in \{0.25, 0.3, 0.35\}$  at  $t = 100$ ; sampling interval  $\Delta t = 2$  and the length of time window  $m = 5$ .

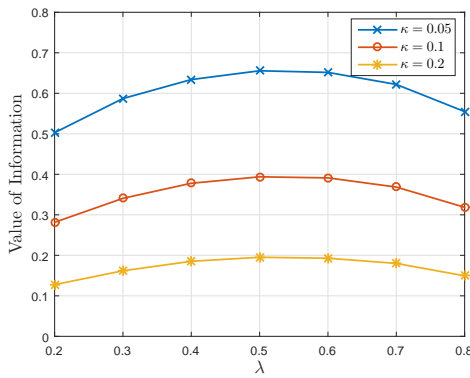


Fig. 7. VoI in the noisy OU process versus the sampling rate  $\lambda$  for  $\kappa \in \{0.05, 0.1, 0.2\}$  at  $t = 100$ ; noise parameter  $\sigma_n^2 = 0.5$  and the length of time window  $m = 2$ .

In Fig. 7, we investigate the effect of the sampling rate and correlation on the VoI in the noisy OU process. Fixing  $\kappa$ , we observe that both small and large sampling rates lead to small VoI. For small  $\lambda$ , the system lacks the newly generated status updates to predict the current status of the underlying random process. For large  $\lambda$ , more status updates have been sampled at the source, but they may not be transmitted in a timely manner because they need to wait for a longer time in the FCFS queue before being transmitted. Fixing  $\lambda$ , the system sees the large value when  $\kappa$  is small. The parameter  $\kappa$  represents the mean reversion which can be used to capture the correlation of the latent OU process. Compared to the less correlated samples (larger  $\kappa$ ), the value of highly correlated samples is larger, which further illustrates that “old” samples from the highly correlated source may still have value in some cases.

Fig. 8 and 9 show the statistical properties of the VoI in the worst case. Fig. 8 shows the density of the discrete path of the worst-case VoI and the theoretical density function given in Proposition 2 when  $\kappa = 0.1$ . It is clear to find that the results obtained from Monte Carlo simulations are consistent with the PDF obtained from the theoretical analysis. In Fig. 9, we plot the CDF of the worst-case VoI given in Proposition 3 for different values of  $\kappa$  and  $\sigma_n^2$ . This figure illustrates that the

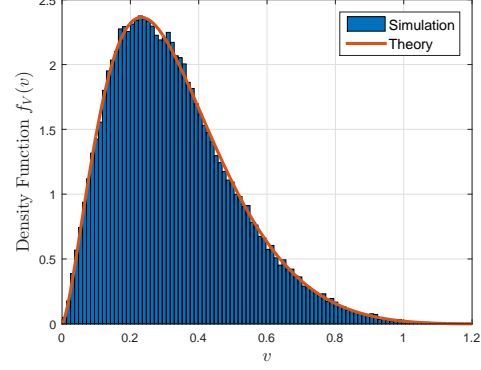


Fig. 8. The density function of the worst-case VoI; correlation parameter  $\kappa = 0.1$ , noise parameter  $\sigma_n^2 = 0.5$  and sampling rate  $\lambda = 0.5$ .

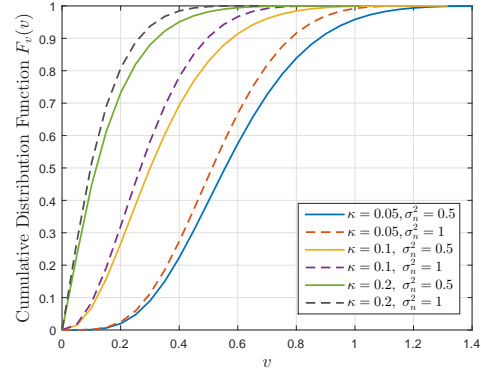


Fig. 9. The cumulative distribution function of the worst-case VoI for  $\kappa \in \{0.05, 0.1, 0.2, 0.3\}$  and  $\sigma_n^2 \in \{0.5, 1\}$ ; sampling rate  $\lambda = 0.5$ .

“VoI outage” is more likely to occur when the status updates are less correlated or the system experiences large noise.

## VII. CONCLUSIONS

In this paper, a mutual-information based value of information framework was formalised to characterise how valuable the status updates are for hidden Markov models. The notion of VoI was interpreted as the reduction in the uncertainty of the current unobserved status given that we have a dynamic sequence of noisy measurements. We took the noisy OU process as an example and derived closed-form VoI expressions. Moreover, the VoI was further explored in the context of the noisy OU model with different sampling policies. For uniform sampling, the simplified VoI expressions were derived in high and low SNR regimes, respectively. For random sampling, the simplified expression and the statistical properties of VoI were obtained. Furthermore, numerical results are presented to verify the accuracy of our theoretical analysis. Compared with the traditional AoI metric, the proposed VoI framework can be used to describe the timeliness of the source data, how correlated the underlying random process is, and the noise in hidden Markov models.

## APPENDIX A PROOF OF PROPOSITION 1

Since  $(\mathbf{Y}^T, X_t)$  is multivariate normal distribution, the VoI defined in (2) can be written as [39]

$$\begin{aligned} v(t) &= I(X_t; \mathbf{Y}^T) \\ &= h(X_t) + h(\mathbf{Y}^T) - h(\mathbf{Y}^T, X_t) \\ &= \frac{1}{2} \log \frac{\text{Var}[X_t] \det(\Sigma_{\mathbf{Y}})}{\det(\Sigma_{\mathbf{Y}, X_t})} \end{aligned} \quad (58)$$

where  $\Sigma_{\mathbf{Y}}$  and  $\Sigma_{\mathbf{Y}, X_t}$  are the covariance matrices of  $\mathbf{Y}$  and  $(\mathbf{Y}^T, X_t)^T$ , respectively.

Since  $\mathbf{X}$  and  $\mathbf{N}$  are independent, the covariance matrix  $\Sigma_{\mathbf{Y}}$  can be given as

$$\Sigma_{\mathbf{Y}} = \Sigma_{\mathbf{X}} + \Sigma_{\mathbf{N}}. \quad (59)$$

Moreover,  $\det(\Sigma_{\mathbf{Y}, X_t})$  in (58) can be obtained by the probability density function of  $(\mathbf{Y}^T, X_t)$ , and this density function can be further obtained by marginalising the joint density function of  $(\mathbf{Y}^T, X_t, \mathbf{X}^T)$  over  $\mathbf{X}^T$ . Hence, we have

$$\det(\Sigma_{\mathbf{Y}, X_t}) = \text{Var}[X_t | X_{t_n}] \det \left( \Sigma_{\mathbf{N}} + \Sigma_{\mathbf{X}} + \frac{\Sigma_{\mathbf{X}} \mathbf{v} \mathbf{v}^T \Sigma_{\mathbf{N}}}{\text{Var}[X_t | X_{t_n}]} \right) \quad (60)$$

where vector  $\mathbf{v} = [0, \dots, 0, e^{-\kappa(t-t_n)}]^T$ .

Substituting (59) and (60) into (58), the VoI for the noisy OU process can be expressed as

$$\begin{aligned} v(t) &= \frac{1}{2} \log \left( \frac{\text{Var}[X_t]}{\text{Var}[X_t | X_{t_n}] \det(\Sigma_{\mathbf{N}} + \Sigma_{\mathbf{X}} + \frac{\Sigma_{\mathbf{X}} \mathbf{v} \mathbf{v}^T \Sigma_{\mathbf{N}}}{\text{Var}[X_t | X_{t_n}]})} \right). \end{aligned} \quad (61)$$

By utilising the matrix determinant lemma, the determinant in the denominator can be written as

$$\begin{aligned} \det \left( \Sigma_{\mathbf{N}} + \Sigma_{\mathbf{X}} + \frac{\Sigma_{\mathbf{X}} \mathbf{v} \mathbf{v}^T \Sigma_{\mathbf{N}}}{\text{Var}[X_t | X_{t_n}]} \right) \\ = \left( 1 + \frac{\mathbf{v}^T (\Sigma_{\mathbf{X}}^{-1} + \Sigma_{\mathbf{N}}^{-1})^{-1} \mathbf{v}}{\text{Var}[X_t | X_{t_n}]} \right) \det(\Sigma_{\mathbf{N}} + \Sigma_{\mathbf{X}}). \end{aligned} \quad (62)$$

Therefore, the VoI expression can be further written as

$$\begin{aligned} v(t) &= \frac{1}{2} \log \left( \frac{1}{1 - e^{-2\kappa(t-t_n)}} \right) \\ &\quad - \frac{1}{2} \log \left( 1 + \frac{2\kappa\sigma_n^2}{\sigma^2 (e^{2\kappa(t-t_n)} - 1)} \frac{\det(\mathbf{A}_{mm})}{\det(\mathbf{A})} \right) \end{aligned} \quad (63)$$

where  $\mathbf{A} = \sigma_n^2 \Sigma_{\mathbf{X}}^{-1} + \mathbf{I}$ .

## APPENDIX B PROOF OF THE DETERMINANT CALCULATION FOR UNIFORM SAMPLING

Let the  $m$ -dimensional circulant matrix  $\boldsymbol{\eta}$  where

$$(\boldsymbol{\eta})_{i,j} = \begin{cases} 1 & i = m, j = 1 \\ 1 & j = i + 1 \\ 0 & \text{others} \end{cases} \quad (64)$$

$$\det(\boldsymbol{\eta}) = (-1)^{m-1}. \quad (65)$$

The product of matrix  $\mathbf{A}$  and  $\boldsymbol{\eta}$  can be partitioned into four blocks

$$\begin{aligned} \mathbf{A}\boldsymbol{\eta} &= \begin{bmatrix} 0 & a & b & 0 & \cdots & 0 \\ 0 & b & c & b & & \\ \vdots & & b & c & \ddots & \\ 0 & & & \ddots & \ddots & b \\ b & & & & b & c \\ a & & & & & b \end{bmatrix} \\ &= \begin{bmatrix} \boldsymbol{\eta}_{11} & \boldsymbol{\eta}_{12} \\ \boldsymbol{\eta}_{21} & \boldsymbol{\eta}_{22} \end{bmatrix}. \end{aligned} \quad (66)$$

Taking the determinant of both side, then we have

$$\det(\mathbf{A}) = \frac{\det(\boldsymbol{\eta}_{22}) \det(\boldsymbol{\eta}_{11} - \boldsymbol{\eta}_{12} \boldsymbol{\eta}_{22}^{-1} \boldsymbol{\eta}_{21})}{\det(\boldsymbol{\eta})}. \quad (67)$$

Here,

$$\det(\boldsymbol{\eta}_{22}) = b^{m-1}. \quad (68)$$

As  $\boldsymbol{\eta}_{22}$  is a tri-band Toeplitz matrix, the inverse matrix can be expressed by [40]

$$\boldsymbol{\eta}_{22}^{-1} = \begin{bmatrix} J_1 & J_2 & \cdots & J_{m-1} \\ & J_1 & \ddots & \vdots \\ & & \ddots & J_2 \\ & & & J_1 \end{bmatrix} \quad (69)$$

where  $J_i$  falls in the form of the following recurrence relation

$$J_i = -\frac{c}{b} J_{i-1} - J_{i-2} \quad (70)$$

with  $J_1 = \frac{1}{b}$  and  $J_2 = -\frac{c}{b^2}$ . Substituting (66), (68) and (69) into (67), we have

$$\det(\mathbf{A}) = (-1)^m b^{m-1} (a^2 J_{m-1} + 2ab J_{m-2} + b^2 J_{m-3}). \quad (71)$$

The recurrence relation can be solved by the roots of the characteristic polynomial. The characteristic equation is given by

$$\lambda^2 + \frac{c}{b} \lambda + 1 = 0, \quad (72)$$

and the eigenvalues are

$$\lambda_1 = \frac{-c + \sqrt{c^2 - 4b^2}}{2b}, \quad \lambda_2 = \frac{-c - \sqrt{c^2 - 4b^2}}{2b}. \quad (73)$$

Thus,  $J_i$  can be written as

$$J_i = \frac{1}{\sqrt{c^2 - 4b^2}} (\lambda_1^i - \lambda_2^i). \quad (74)$$

Substituting  $J_i$  into (71), we obtain the result given in (22). The result given in (23) can be obtained in the similar way.

## APPENDIX C PROOF OF LEMMA 1

Mathematical induction is utilised to prove the statement  $f_k$  for all natural numbers  $1 \leq k \leq m$ .

First, for the base case, we have

$$f_1 = 1 + \frac{1}{\gamma} a_1, \quad f_1 = 0 \cdot 1 + a_1 \frac{1}{\gamma} + \frac{1}{\gamma^2}. \quad (75)$$

$$\begin{aligned} f_2 &= \left(\frac{1}{\gamma}a_1 + 1\right)\left(\frac{1}{\gamma}a_2 + 1\right) - \frac{1}{\gamma^2}b_1^2, \\ f_2 &= 1 + (a_1 + a_2)\frac{1}{\gamma} + (a_1a_2 - b_1^2)\frac{1}{\gamma^2}. \end{aligned} \quad (76)$$

It is easy to see that  $f_1$  and  $f_2$  are clearly true.

Next, we turn to the induction hypothesis. We assume that, for a particular  $s$ , the cases  $k = s$  and  $k = s + 1$  hold. This means that

$$\begin{aligned} f_s &= 1 + \sum_{i=1}^s a_i \frac{1}{\gamma} + \left( \sum_{1 \leq i < j \leq s} a_i a_j - \sum_{i=1}^{s-1} b_i^2 \right) \frac{1}{\gamma^2} + O\left(\frac{1}{\gamma^3}\right) \\ f_{s+1} &= \\ 1 + \sum_{i=1}^{s+1} a_i \frac{1}{\gamma} + \left( \sum_{1 \leq i < j \leq s+1} a_i a_j - \sum_{i=1}^s b_i^2 \right) \frac{1}{\gamma^2} + O\left(\frac{1}{\gamma^3}\right). \end{aligned} \quad (77)$$

As matrix  $\mathbf{A}$  is tridiagonal, the cofactor expansion can be used to calculate the determinant. When  $k = s + 2$ , we have the following recurrence relation

$$f_{s+2} = \left(\frac{1}{\gamma}a_{s+2} + 1\right)f_{s+1} - \frac{1}{\gamma^2}b_{s+1}^2 f_s. \quad (78)$$

Substituting (77) into (78), we have

$$\begin{aligned} f_{s+2} &= \left(a_{s+2} \sum_{i=1}^{s+1} a_i + \sum_{1 \leq i < j \leq s+1} a_i a_j - \sum_{i=1}^s b_i^2\right) \frac{1}{\gamma^2} \\ &\quad + \left(a_{s+2} + \sum_{i=1}^{s+1} a_i\right) \frac{1}{\gamma} + 1 + \frac{1}{\gamma^2}b_{s+1}^2 + O\left(\frac{1}{\gamma^3}\right) \\ &= 1 + \sum_{i=1}^{s+2} a_i \frac{1}{\gamma} + \left(\sum_{1 \leq i < j \leq s+2} a_i a_j - \sum_{i=1}^{s+1} b_i^2\right) \frac{1}{\gamma^2} + O\left(\frac{1}{\gamma^3}\right). \end{aligned} \quad (79)$$

This shows that the statement  $f_{s+2}$  also holds true, establishing the inductive step.

Both base cases and inductive steps are proved to be true, therefore we can conclude that  $f_k$  in (40) holds for every  $k$  with  $1 \leq k \leq m$ .

## APPENDIX D

### PROOF OF THE JOINT DENSITY FUNCTION OF SAMPLING INTERVAL AND SYSTEM TIME

In the FCFS M/M/1 queueing system, the variables  $S_n$ ,  $W_{n+1}$  and  $T_{n+1}$  are independent with each other, thus their joint PDF can be obtained by

$$\begin{aligned} f_{S_n, W_{n+1}, T_{n+1}}(s_n, w, t) &= f_{S_n}(s_n)f_W(w)f_T(t) \\ &= \lambda\mu(\mu - \lambda)e^{-\lambda t - \mu w - (\mu - \lambda)s_n}. \end{aligned} \quad (80)$$

The system time of the  $(n+1)$ th update  $S_{n+1}$  can be expressed by

$$S_{n+1} = (S_n - T_{n+1})^+ + W_{n+1} \quad (81)$$

where the non-negative term represents the waiting time. Therefore, the joint PDF of  $T_{n+1}$  and  $S_{n+1}$  can be obtained by

$$\begin{aligned} f_{T, S}(t, s) &= \int_0^{+\infty} f_{S_n, W, T}(s_n, s - (s_n - t)^+, t) ds_n \\ &= \lambda\mu(\mu - \lambda)e^{-\lambda t} \left( \int_0^t e^{-\mu s - (\mu - \lambda)s_n} ds_n \right. \\ &\quad \left. + \int_t^{s+t} e^{-\mu(s+s_n+t) - (\mu - \lambda)s_n} ds_n \right) \\ &= \lambda\mu e^{-\lambda t - \mu s} - \mu^2 e^{-\mu(t+s)} + \mu(\mu - \lambda)e^{-\mu t - (\mu - \lambda)s}. \end{aligned} \quad (82)$$

## REFERENCES

- [1] S. Kaul, R. Yates, and M. Gruteser, "Real-time status: How often should one update?" in *2012 Proceedings IEEE INFOCOM*, 2012, pp. 2731–2735.
- [2] R. D. Yates and S. Kaul, "Real-time status updating: Multiple sources," in *2012 IEEE International Symposium on Information Theory Proceedings*, 2012, pp. 2666–2670.
- [3] A. Kosta, N. Pappas, and V. Angelakis, *Age of Information: A New Concept, Metric, and Tool*. Now Foundations and Trends, 2017.
- [4] M. A. Abd-Elmagid, N. Pappas, and H. S. Dhillon, "On the role of age of information in the Internet of Things," *IEEE Communications Magazine*, vol. 57, no. 12, pp. 72–77, 2019.
- [5] R. D. Yates and S. K. Kaul, "The age of information: Real-time status updating by multiple sources," *IEEE Transactions on Information Theory*, vol. 65, no. 3, pp. 1807–1827, 2019.
- [6] Y. Inoue, H. Masuyama, T. Takine, and T. Tanaka, "A general formula for the stationary distribution of the age of information and its application to single-server queues," *IEEE Transactions on Information Theory*, vol. 65, no. 12, pp. 8305–8324, 2019.
- [7] S. K. Kaul, R. D. Yates, and M. Gruteser, "Status updates through queues," in *2012 46th Annual Conference on Information Sciences and Systems (CISS)*, 2012, pp. 1–6.
- [8] A. M. Bedewy, Y. Sun, and N. B. Shroff, "Minimizing the age of information through queues," *IEEE Transactions on Information Theory*, vol. 65, no. 8, pp. 5215–5232, 2019.
- [9] ———, "Age-optimal information updates in multihop networks," in *2017 IEEE International Symposium on Information Theory (ISIT)*, 2017, pp. 576–580.
- [10] S. K. Kaul and R. D. Yates, "Age of information: Updates with priority," in *2018 IEEE International Symposium on Information Theory (ISIT)*, 2018, pp. 2644–2648.
- [11] C. Kam, S. Kompella, G. D. Nguyen, J. E. Wieselthier, and A. Ephremides, "On the age of information with packet deadlines," *IEEE Transactions on Information Theory*, vol. 64, no. 9, pp. 6419–6428, 2018.
- [12] ———, "Controlling the age of information: Buffer size, deadline, and packet replacement," in *MILCOM 2016 - 2016 IEEE Military Communications Conference*, 2016, pp. 301–306.
- [13] Q. He, D. Yuan, and A. Ephremides, "Optimal link scheduling for age minimization in wireless systems," *IEEE Transactions on Information Theory*, vol. 64, no. 7, pp. 5381–5394, 2018.
- [14] Z. Wang, X. Qin, B. Liu, and P. Zhang, "Joint data sampling and link scheduling for age minimization in multihop cyber-physical systems," *IEEE Wireless Communications Letters*, vol. 8, no. 3, pp. 765–768, 2019.
- [15] X. Wu, J. Yang, and J. Wu, "Optimal status update for age of information minimization with an energy harvesting source," *IEEE Transactions on Green Communications and Networking*, vol. 2, no. 1, pp. 193–204, 2018.
- [16] E. Gindullina, L. Badia, and D. Gündüz, "Age-of-information with information source diversity in an energy harvesting system," 2020.
- [17] M. A. Abd-Elmagid and H. S. Dhillon, "Average peak age-of-information minimization in UAV-assisted IoT networks," *IEEE Transactions on Vehicular Technology*, vol. 68, no. 2, pp. 2003–2008, 2019.
- [18] Z. Jia, X. Qin, Z. Wang, and B. Liu, "Age-based path planning and data acquisition in UAV-assisted IoT networks," in *2019 IEEE International Conference on Communications Workshops (ICC Workshops)*, 2019, pp. 1–6.

- [19] M. A. Abd-Elmagid, A. Ferdowsi, H. S. Dhillon, and W. Saad, "Deep reinforcement learning for minimizing age-of-information in UAV-assisted networks," in *2019 IEEE Global Communications Conference (GLOBECOM)*, 2019, pp. 1–6.
- [20] W. Li, L. Wang, and A. Fei, "Minimizing packet expiration loss with path planning in UAV-assisted data sensing," *IEEE Wireless Communications Letters*, vol. 8, no. 6, pp. 1520–1523, 2019.
- [21] J. Hu, H. Zhang, L. Song, R. Schober, and H. V. Poor, "Cooperative Internet of UAVs: Distributed trajectory design by multi-agent deep reinforcement learning," *IEEE Transactions on Communications*, vol. 68, no. 11, pp. 6807–6821, 2020.
- [22] Y. Sun and B. Cyr, "Sampling for data freshness optimization: Non-linear age functions," *Journal of Communications and Networks*, vol. 21, no. 3, pp. 204–219, 2019.
- [23] Y. Sun, E. Uysal-Biyikoglu, R. D. Yates, C. E. Koksal, and N. B. Shroff, "Update or wait: How to keep your data fresh," *IEEE Transactions on Information Theory*, vol. 63, no. 11, pp. 7492–7508, 2017.
- [24] X. Zheng, S. Zhou, Z. Jiang, and Z. Niu, "Closed-form analysis of non-linear age of information in status updates with an energy harvesting transmitter," *IEEE Transactions on Wireless Communications*, vol. 18, no. 8, pp. 4129–4142, 2019.
- [25] A. Kosta, N. Pappas, A. Ephremides, and V. Angelakis, "The cost of delay in status updates and their value: Non-linear ageing," *IEEE Transactions on Communications*, vol. 68, no. 8, pp. 4905–4918, 2020.
- [26] C. Kam, S. Komella, G. D. Nguyen, J. E. Wieselthier, and A. Ephremides, "Towards an effective age of information: Remote estimation of a Markov source," in *IEEE INFOCOM 2018 - IEEE Conference on Computer Communications Workshops (INFOCOM WK-SHPS)*, 2018, pp. 367–372.
- [27] Y. Sun, Y. Polyanskiy, and E. Uysal, "Sampling of the Wiener process for remote estimation over a channel with random delay," *IEEE Transactions on Information Theory*, vol. 66, no. 2, pp. 1118–1135, 2020.
- [28] T. Z. Ornee and Y. Sun, "Sampling for remote estimation through queues: Age of information and beyond," in *2019 International Symposium on Modeling and Optimization in Mobile, Ad Hoc, and Wireless Networks (WiOPT)*, 2019, pp. 1–8.
- [29] X. Zheng, S. Zhou, and Z. Niu, "Urgency of information for context-aware timely status updates in remote control systems," *IEEE Transactions on Wireless Communications*, vol. 19, no. 11, pp. 7237–7250, 2020.
- [30] J. Hribar, M. Costa, N. Kaminski, and L. A. DaSilva, "Updating strategies in the Internet of Things by taking advantage of correlated sources," in *GLOBECOM 2017 - 2017 IEEE Global Communications Conference*, 2017, pp. 1–6.
- [31] R. Singh, G. K. Kamath, and P. R. Kumar, "Optimal information updating based on value of information," in *2019 57th Annual Allerton Conference on Communication, Control, and Computing (Allerton)*, 2019, pp. 847–854.
- [32] T. Soleymani, S. Hirche, and J. S. Baras, "Optimal self-driven sampling for estimation based on value of information," in *2016 13th International Workshop on Discrete Event Systems (WODES)*, 2016, pp. 183–188.
- [33] Y. Sun and B. Cyr, "Information aging through queues: A mutual information perspective," in *2018 IEEE 19th International Workshop on Signal Processing Advances in Wireless Communications (SPAWC)*, 2018, pp. 1–5.
- [34] Z. Wang, M. A. Badiu, and J. P. Coon, "A value of information framework for latent variable models," in *GLOBECOM 2020 - 2020 IEEE Global Communications Conference*, 2020, pp. 1–6.
- [35] B. Allévius, "On the precision matrix of an irregularly sampled AR(1) process," 2018.
- [36] Y. Wei, X. Jiang, Z. Jiang, and S. Shon, "Determinants and inverses of perturbed periodic tridiagonal Toeplitz matrices," *Advances in Difference Equations*, vol. 2019, no. 1, p. 410, 2019.
- [37] H. Rue and L. Held, *Gaussian Markov random fields: theory and applications*. CRC press, 2005.
- [38] A. Papoulis, *Probability, random variables, and stochastic processes*. McGraw-Hill, 1991.
- [39] T. M. Cover and J. A. Thomas, *Elements of Information Theory*. John Wiley & Sons, 2006.
- [40] B. Zuo, Z. Jiang, and D. Fu, "Determinants and inverses of Ppoelitz and Ppankel matrices," *Special Matrices*, vol. 6, no. 1, pp. 201–215, 2018.